Chemically tagging the HR1614 moving group

G.M. De Silva[1] and K.C. Freeman

Mount Stromlo Observatory, Australian National University, Weston ACT 2611, Australia

gayandhi@mso.anu.edu.au

J. Bland-Hawthorn

Anglo-Australian Observatory, Eastwood NSW 2122, Australia

jbh@aao.gov.au

M. Asplund and M.S. Bessell

Mount Stromlo Observatory, Australian National University, Weston ACT 2611, Australia

ABSTRACT

We present abundances for a sample of F,G,K dwarfs of the HR1614 moving group based on high resolution, high S/N ratio spectra from AAT/UCLES. Our sample includes stars from Feltzing & Holmberg (2000), as well as from Eggen (1998). Abundances were derived for Na, Mg, Al, Si, Ca, Mn, Fe, Ni, Zr, Ba, Ce, Nd, and Eu. The alpha, Fe, and Fe-peak element abundances show a bimodal distribution, with four stars having solar metallicities while the remaining 14 stars are metal rich [Fe/H] $\geq$ 0.25 dex. However the abundances of these two groups converge for the heavier n-capture elements. Based on their photometry and kinematics, three of the four deviating stars are likely non-members or binaries. Although one star cannot be excluded on these grounds, we do expect low-level contamination from field stars within the HR1614 moving group's range of magnitude, color and space velocities.

Disregarding these four stars, the abundance scatter across the group members for all elements is low. We find that there is an 80% probability that the intrinsic scatter does not exceed the following values: Fe 0.01; Na 0.08; Mg 0.02; Al 0.06; Si 0.02; Ca 0.02; Mn 0.01; Ni 0.01; Zr 0.03; Ba 0.03; Ce 0.04; Nd 0.01 and Eu 0.02 dex. The homogeneity of the HR 1614 group in age and abundance

[1]Now at European Southern Observatory, Alonso de Cordova 3107, Casilla 19001, Santiago 19, Chile

suggests that it is the remnant of a dispersed star-forming event. Its kinematical coherence shows that such a dispersing system need not be significantly perturbed by external dynamical influences like galactic spiral structure or giant molecular clouds, at least over a period of 2 Gyr.

Subject headings: Galaxy: evolution — Galaxy: open clusters and associations: individual(HR1614 moving group) — stars: abundances

1. Introduction

The concept of moving groups was first introduced by Olin Eggen in the 1960s. Basically the stars form from a common progenitor gas cloud. As the cluster disperses around the Galaxy, it stretches into a tube-like structure around the Galactic plane and after several Galactic orbits it will dissolve into the Galactic background. If the Sun happens to be inside this tube, the member stars will appear all over the sky but may be identified as a group through their common space velocities. A moving group is therefore the in-between step from bound clusters to field stars.

For this reason moving groups are an important class of objects for the purpose of testing the chemical tagging technique put forward by Freeman & Bland-Hawthorn (2002). In summary, the long term goal of chemical tagging is to reassemble the ancient star-forming aggregates in the Galactic disk by studying their chemical signatures, in order to unravel the sequence of events involved in the dissipative formation of the disk. One of the fundamental requirements for the viability of chemical tagging is chemical homogeneity within individual Disk clusters. Since most bound open clusters are believed to be chemically homogeneous (eg. Hyades (De Silva et al. 2006b) and Collinder 261 (De Silva et al. 2006a)), establishing homogeneity in unbound moving groups which retain some kinematical identity is the next step for the chemical tagging technique. The final step is to chemically identify groups which have no dynamical identity.

Although the existence of many stellar moving groups has been suggested, the reality of most is yet to be verified. In the past due to the lack of accurate parallaxes it has been difficult to reliably identify the stellar members of moving groups. This has now been partly overcome from the observations by the Hipparcos satellite. The presence of a moving group associated with the star HR1614, first advocated by Eggen (1978a), was verified by Feltzing & Holmberg (2000) using the new Hipparcos parallaxes and recent radial velocities, and

provides an extended sample of stellar members.

Eggen's initial identification of the moving group came from studying a sample of stars within $\pm$ 10km s^{-1} of the galactic rotational velocity (V) of star HR1614. He used the high excess in $b-y$ as a membership criterion for his stars to obtain a color-magnitude diagram (Eggen 1978b, Fig 1a.) resembling that of an old open cluster. Based on a few spectroscopic studies and positions in the M_V vs. $R-I$ color-magnitude diagram, Eggen (1978b) concluded that the majority of stars he classified as members were as metal rich as the Hyades.

Followup studies by Smith (1983) using DDO photometry showed enhanced cyanogen bands in Eggen (1978a) sample stars. The derived metallicity confirmed Eggen's estimate of a high metallicity, but two giants found to have significantly low metallicity cast doubt over Eggen's $b-y$ membership criteria. Enforcing a strict criterion using UBV, DDO and $b-y$, Smith (1983) showed that many of Eggen's original candidates did not belong to the group. Eggen (1992), utilizing the CN-enhancement, provided a second sample of main sequence dwarfs with the same V-velocity restrictions as applied earlier. With the accurate parallax measurements made available from the Hipparcos mission, Eggen (1998) showed that the group membership for his HR1614 sample (Eggen 1992) is supported by Hipparcos parallaxes. However for two stars where the discrepancies were large, Eggen (1998) suggested errors in the Hipparcos parallaxes.

Feltzing & Holmberg (2000, hereafter FH) utilized Hipparcos parallaxes and radial velocities from several recent catalogues to perform an unbiased search for HR1614 member stars over a large region of UV space. They conclude that there is a distinct stellar population of metal rich stars centered at U = 10 km s^{-1}, V = -60 km s^{-1} and tilted in the UV plane, which they associate with the HR1614 moving group. Following simulations by Skuljan et al. (1997) and their own basic simulations, FH find the observed tilt in the UV plane to be a feature of a moving group. In contrast, the classical criteria used by Eggen (based on epicyclic theory), requires all member stars to lie at constant V in the UV plane. FH state that such central clumping will only occur if the Sun is located very close to the center of the moving group, otherwise a tilt is to be expected.

With the past literature pointing towards its reality, the HR1614 moving group is an attractive target for testing chemical tagging. The star cluster is quite distinctive due to its age of about 2 Gyr, and high metallicity of [Fe/H]= +0.25. Its the stellar motions suggest that these stars formed in the inner disk. Dehnen (1999) (see also Raboud et al. 1998), shows

that there is an overdensity in the UV plane at U = -20 $\mathrm{km\,s^{-1}}$ and V = -45 $\mathrm{km\,s^{-1}}$ (earlier named the U-anomaly), which he associates with stars thrown out from the inner disk, an effect particularly strong close to the Galactic bars' outer Lindblad resonance, where the Sun is located outside the outer Lindblad resonance. Its likely origin in the inner disk makes the HR1614 moving group of particular interest. It gives us a unique chance to test chemical tagging precepts on stars that originated away from the solar circle. The HR1614 moving group has never been subject to a high resolution abundance study. We have now for the first time performed a detailed abundance analysis.

2. Observations

The original data were obtained at the 4m AAT, using UCLES in August 2003. Observations were done at two wavelength settings at the blue and red. The blue setting was centered at 4130Å and covers the region from 3800Å to 4700Å, while the red setting was centered at 7040Å covering the spectral range from 5510Å to 10200Å. The 31.6 lines $\mathrm{mm^{-1}}$ echelle grating was always used. The slit was opened to a width of 1.2 arcsecs on the sky providing a resolving power of 48,000.

The observing routine included 10 bias frames, and 5 quartz lamp exposures to provide data for flat fielding, taken at the start of each night. A Th-Ar hollow cathode lamp spectra was taken before and after each stellar exposure. Two radial velocity standards, one at the start and one at the end of each night, were also observed. The stellar exposures were taken in batches of at least 3 exposures per star, with each exposure typically around 200 secs. All program stars have a total signal-to-noise ratio greater than 150 per pixel at the central wavelengths.

The spectroscopic data were reduced using the IRAF packages IMRED, CCDRED, and ECHELLE. The preliminaries included biasing, flat fielding, scattered light removal, order extraction, wavelength calibration and continuum fitting. Details of the final sample selected for abundance analysis are given in Table 1.

3. Abundance analysis

3.1. Model Atmospheres and Spectral Lines

The abundance analysis makes use of the latest version of the MOOG code (Sneden 1973) for LTE EW analysis and spectral syntheses. Interpolated Kurucz model atmospheres based on the ATLAS9 code (Castelli et al. 1997) with no convective overshoot were used throughout this study.

Now we focus on the lines of Na, Mg, Al, Si, Ca, Mn, Ni, Fe, Zr, Ba, Ce, Nd, and Eu. A full line list is given in Table 2 as well as EWs of the reference star. The gf values for the detected lines of Na, Mg, Al, Si, Ca, Ni, and Zr were obtained from a combination of lines from Allende Prieto et al. (2004); Yong et al. (2005); Reddy et al. (2003) and Paulson et al. (2003). For Mn, the gf values were taken from Prochaska & McWilliam (2000) and include the effects of hyperfine splitting. The main sources of the Fe I line data is the laboratory measurements by the Oxford group (Blackwell et al., 1979a,b, 1995 and references therein). This was supplemented by additional lines from Reddy et al. (2003). For Fe II we adopt the gf values from Biemont et al. (1991); Paulson et al. (2003) and Allende Prieto et al. (2002). The only measurable Zr line data was obtained via the Viena Atomic Line Database (VALD[1]; Kupka et al. (2000, 1999); Ryabchikova et al. (1997); Piskunov et al. (1995)), from the Bell heavy database (Kurucz CD-ROM 18, 1993). Ba gf values were adopted from Prochaska et al. (2000) as well as Allende Prieto et al. (2004). The Ce gf values were obtained from the Database on Rare Earths At Mons University (DREAM[2]; Biemont et al. (1999)). The gf values for Nd were taken from Den Hartog et al. (2003), and finally, the Eu gf values were taken from Lawler et al. (2001) and we account for hyperfine splitting and isotopic shifts assuming a solar isotopic mix.

3.2. Stellar parameters

Initially T_{eff} was estimated using the color-temperature relations of Alonso et al. (1996), equation (7) and (8), using V-K values where the K magnitudes were obtained from 2MASS and adopting [Fe/H] = +0.2. These temperature estimates were used as an initial guess

[1]http://ams.astro.univie.ac.at/vald/

[2]http://w3.umh.ac.be/ astro/dream.shtml

when deriving spectroscopic temperatures. An estimate of log g was then obtained using the distances (from Hipparcos parallaxes), bolometric corrections, and stellar mass from Bertelli et al. (1994) isochrones. The best fitting isochrone was found to be of age ≈ 2 Gyr, consistent with the estimate obtained by FH. Figure 1 shows our sample of stars overlaid with several isochrones for Z = 0.05.

Next we derived the stellar parameters based on spectroscopy. We compute abundances for all Fe I and Fe II lines based on the measured EW. The EWs were measured by fitting a Gaussian profile to each line using the interactive *SPLOT* function in IRAF. T_{eff} was derived by forcing the Fe I abundances to be independent of excitation potential, ie. excitational equilibrium. Microturbulence was derived from the condition that Fe I lines show no abundance trend with EW. Log g was derived via ionization equilibrium, ie. the abundances from Fe I equals Fe II. The photometric estimates of T_{eff} and log g were used as the initial guess model and iterated until a self consistent set of model parameters were obtained. The spectroscopic estimates of T_{eff} are hotter than the photometric estimates on average by 150 K. For our abundance analysis we adopt the spectroscopic stellar parameters. Table 3 lists the adopted parameters.

3.3. Elemental Abundances

Depending on the degree of blending of the spectral lines, abundances were derived either by EW measurements or by spectral synthesis. The EW measurements were used for abundance determinations for all elements, except the heavy elements from Ba to Eu, which required full spectral synthesis.

In our initial analysis, we derived absolute abundances, but for the purposes of testing chemical tagging, we decided to use differential abundances as these were found to have smaller systematic errors. The final differential abundances Δ[X/H] were derived by subtracting the absolute abundance of each individual line of the reference star HR1614 from the same line in the sample stars, and then taking the mean of the differences for each element. By using such a line-by-line differential technique we can identify and remove any problematic lines, reducing the errors due to the uncertainty in the line data, hence minimizing the star-to-star scatter. The differential Fe abundances Δ[Fe/H] is plotted in Fig 2. The differential abundances for all elements lighter than Fe are plotted in Fig 3 and those heavier than Fe are plotted in Fig 4. Note that the zero level in these plots do not correspond to the

solar metallicity, as these are plots of the differential abundances relative to HR1614. Also, note that four stars (HIP 13513, HIP6762, HIP 25840, HIP 116970) were found to have solar-level abundances for all elements except for the heavier n-capture elements. These stars are identified in the plots with different symbols. We will discuss our results and these deviating stars in detail in Section 5.1. The derived absolute abundances (log ϵ) of the sample stars are presented in Table 4.

3.4. Error Analysis

The main sources of error in the present study are that of EW measurements, continuum placement and stellar parameters. Because we are only interested in the differential abundances, external errors, such as uncertainties in the line data and model atmospheres are the least sources of error. The number of lines used to calculate the final abundances also contributed to the total uncertainty for each element.

The error in EWs was estimated by repeated measurements of each line. The measurement errors for the synthesized abundances were derived by changing the abundance until there is a clear visible deviation from the best fit. The error in the stellar parameters were estimated to be δT_{eff} = 50K, δlog g = 0.1 cm s^{-2} and $\delta\xi$ = 0.1 km s^{-1} based on our spectroscopic derivation . Table 5 summarizes the abundance sensitivities to each stellar parameter and methods of derivation for two stars at either end of the temperature range. Typical values of the final error is as follows; Fe = 0.05 dex, Na = 0.07 dex, Mg = 0.07 dex, Al = 0.07 dex, Si = 0.05 dex, Ca = 0.07 dex, Mn = 0.04 dex, Ni = 0.06 dex, Zr = 0.07 dex, Ba = 0.05 dex, Ce = 0.03 dex, Nd = 0.03 dex and Eu = 0.03 dex.

The four stars that show solar-level metallicities in the lighter elements were re-assessed to check whether the stellar parameters or other systematic parameters were at fault. However this was not found to be the case, with large changes in the model parameters (δT$_{eff} \geq$ 300 K, δlog $g \geq 2$, and $\delta\xi \geq 1$) needed to bring these star's abundances in line with the other enriched stars. In conclusion, we find that systematic error is unlikely to explain the behavior of these four stars.

4. Dynamical Analysis

4.1. Membership Criteria

While open cluster members are easily determined from radial velocities with errors less than a few kilometers per second, moving group membership is based on UVW space motion, but the exact criteria for selecting members remain somewhat uncertain.

Eggen's method of isolating moving group members required all member stars to have the same V-velocity, ie. in the direction of the Galactic rotation. In the epicycle approximation, as a star orbits around the Galaxy, it travels on an epicycle about the circular guiding center of its Galactic orbit. If member stars, which would have originated from the one location, are now in the solar neighborhood, within the observable horizon, then this limits their guiding center radii to be very close to that of the Sun. Those member stars with longer and shorter guiding center radii would be either ahead or lag behind the Sun and therefore not be within a small locally defined volume. This means that HR 1614 group member stars located within a small volume should have a similar V-velocity. Any scatter in V would reflect the scatter in the orbital radii. This variation cannot be large for stars within a small volume.

Work by FH and Skuljan et al. (1997) show that such a clump in the UV space is not necessary for all members of the moving group. Their modeling shows that a small *tilt* in the UV space is the dynamical signature of the moving group. This seems to be in contradiction with the above mentioned concept, and is primarily due to the limitations of the epicyclic approximation, but it does mean that the true kinematical signature of moving groups remain uncertain. The sample selected for our chemical analysis includes stars selected from Eggen (via the V-clump criteria) as well as from the FH sample (selected via the tilted criteria). As establishing accurate membership is a key component of our study, obtaining reliable velocity information is essential. While some velocity information is available from the literature, we have decided to undertake our own measurements in order to obtain a consistent set of velocities.

4.2. Radial velocities

Radial velocities (RVs) were determined by Fourier transform cross correlation of template spectra with observed spectra, making use of the packages RVSAO / XCSAO (Kurtz

& Mink 1998; Kurtz et al. 1992) that are run under IRAF. From the available spectra, RVs were estimated using the blue region from 4200 - 4400 Å and the red region from 8465 - 8680 Å , although the red region containing the calcium triplet was given a higher weighting. Template spectra from Zwitter et al. (2004) were obtained via private communication from M. Williams. Since the stellar parameters were already established from our earlier spectroscopic studies, templates matching closest to the sample parameters were selected for the cross correlation.

The procedure undertaken to determine RV was as follows. The barycentric velocity correction was applied to all observed stars using the IRAF package BCVCORR. The data files were then re-sampled according to the template sampling, which had a resolution of 20,000. The continuum normalization of the data were rechecked to ensure almost complete flatness. The template files were cropped to the wavelength ranges of the observed data. Since the observed echelle spectra has inter-order gaps in the red region, the red templates were split into two separate regions according to the available observed spectral windows. The two regions were from 8465 - 8550 Å and 8593 - 8680 Å which included all three of the Ca II triplet lines. For all cross correlations, the apodizing option in XCSAO was turned on to smooth the edges (up to 5% of the spectra) to zero by multiplication with a cosine bell function. Bandpass filtering was set with the parameters low-bin and top-low for low frequency cut-offs, and parameters top-run and nrun to filter the high frequencies. The data was rebinned to 2048 bins set by ncol. By experimentation, the low frequency cut-offs were set to [4,20] which allows the broader spectral features through, while filtering out any residual low frequency structure in the continuum. For the high frequencies, we set the cut-offs to [240,580] after several experimentations to avoid suppressing any line features and ensuring all high signal data passes through, while the high noise regions are removed.

Resulting radial velocity values were selected based on the goodness-of-fit parameter (R) as output from XCSAO. The highest R value for all program stars were over 20 in the blue spectral region and over 30 in the red. While both red and blue regions gave very similar results, the final radial velocities are an average of both the red and blue regions, with a weighting of 3:2 in favor of the red region based on the R values. The exception to this is the star HIP13513, which we measure to have a variable RV with an RV of 3.5 $\mathrm{km\,s^{-1}}$ in the red and -46.9 $\mathrm{km\,s^{-1}}$ in the blue, which was taken at a later date. Note that this star is one of the chemically deviating stars mentioned in Section 3.3. We will discuss these stars later in Section 5.2. With the exception of HIP13513, our results agree better with the measurements by Nordström et al. (2004, N04) where the average difference is about 0.4 $\mathrm{km\,s^{-1}}$, than for FH where the average difference is about 4 $\mathrm{km\,s^{-1}}$, although they

agree within the given error bars of the FH sources. Our RVs for all sample stars and RV standards, as well as several literature values, are listed in Table 6. Our errors as calculated by XCSAO are less than 1 $\mathrm{km\,s^{-1}}$.

4.3. U V W velocities

Using the above computed RVs, and proper motions and parallaxes from Hipparcos, we calculated UVW space velocities making use of the conversion code obtained via private communication from M. Williams. The resulting velocities are with respect to the LSR adopting the standard solar motion of U = 10 $\mathrm{km\,s^{-1}}$, V = 5 $\mathrm{km\,s^{-1}}$, and W = 7 $\mathrm{km\,s^{-1}}$ (Dehnen & Binney 1998). Table 7 lists our derived velocities, as well as those from FH. Overall our velocities are in good agreement with FH with mean differences of about 1.7, 0.6, and 2.1 $\mathrm{km\,s^{-1}}$ in U, V and W respectively.

Figure 5 shows the position of our stars in the UV plane using the new velocities obtained in this study. The presence of a slight slope seems to support the tilted membership criterion argued by FH. By fitting a least squares regression line of the form, V = a + bU, we find a = -55.06 and b = 0.18. The significance of this slope depends on the measurement errors. Taking into account errors in RV's and Hipparcos parallaxes, our typical errors are < 2 $\mathrm{km\,s^{-1}}$ for U, < 10 $\mathrm{km\,s^{-1}}$ for V and < 5 $\mathrm{km\,s^{-1}}$ for W. Considering the uncertainty in the V-velocity to be on average 6 $\mathrm{km\,s^{-1}}$ and disregarding the small uncertainty in U-velocity, we derive the uncertainty in the gradient (b) of the best fitting line to be $\pm$ 0.05. Therefore the slight tilt in Figure 5 is marginally significant and lends support to FH's tilted membership criterion in the UV plane. We will discuss the issue of membership in detail in Section 5.2.

5. Discussion

5.1. Chemical Homogeneity

We have studied a total of 18 stars that were thought to be members following the kinematical criteria of FH and Eggen (1998). Out of this sample, four stars are found to deviate from the cluster mean in all elements except the n-capture elements. Disregarding these four stars for the moment, our abundance analysis demonstrates that the moving group is chemically enriched with mean [Fe/H] = 0.25 adopting a solar value of 7.52 (Sneden et al. 1992), comparable to the result obtained by FH using photometric techniques given the estimated

errors. Table 8 summarizes the cluster mean abundances for all studied elements and the rms scatter, both including and excluding the four deviating stars.

Disregarding the four deviating stars, Table 9 summarizes the intrinsic star-to-star scatter σ_{int} within the HR1614 moving group. By examining the uncertainties in our abundance error analysis we also calculate the uncertainty of the estimated intrinsic scatter. Assuming our abundance measurements follow a Gaussian distribution we estimate the confidence interval for the uncertainty in intrinsic scatter. Taking into account the sampling error in the observed scatter and a 10% uncertainty in our adopted measurement errors, we find that the stated uncertainty limits in Table 9 are approximately 80% confidence limits for σ_{int}. Further, based on a χ^2 analysis we derive the probability of finding the observed scatter given the measurement errors and zero intrinsic scatter. Figure 6 plots this probability for the different elements.

The above analysis does not include the four deviating stars. Since our aim is to obtain an estimate of the level of chemical homogeneity in all the moving group members, it is important for us to determine the nature of the deviating stars. If they are found to be non-members or peculiar in some way (including binary systems, where the original birth abundance level may have been modified), then the level of homogeneity observed is indeed very high. If there is a reason to include the deviating stars, the mean level of homogeneity will rise to well over 0.1 dex. However given the clear bimodality of the results, it seems likely that these stars have a different origin.

5.2. Stellar Membership

Following the bimodal nature of the chemical analysis results, one immediately wonders if the deviating stars are non-members of the group. This is much harder to establish for a moving group than for a bound cluster system. Putting aside any chemical knowledge, space velocities and color-magnitude criteria are the key to establishing membership. If we are to use the tilted criteria of FH, we see in Figure 5 that the deviating star HIP25840 lie outside their tilted boundary. Also adopting Eggen's criteria, this star is below the V-velocity clump. This velocity deviation would be sufficient to class this star as a non-member of the moving group. So we feel justified in excluding this star from further discussion.

Our radial velocity measurements found HIP13513 to have a variable radial velocity. The red and blue spectra were observed a few weeks apart, and the derived RV were greatly different. This prompted a search for established binarity for these four deviating stars. Searching the Hipparcos catalogue confirmed that stars HIP13513 and HIP6762 were binary stars. This would be a valid reason for us to discard these stars in our search for chemical homogeneity.

The stars' position in the CMD also help identify possible non-members. Figure 7 shows the CMD of our sample stars with the deviating stars marked with their respective symbols. HIP25840 and HIP6762 lie clearly away from the main sequence, providing further reason to discard these stars as possible non-members or binaries. HIP13513 happens to lie on the main sequence, however given our earlier discussion on its variability, its positioning on the CMD is likely to be by chance.

Our investigation fails to identify star HIP116970 as a non-member or peculiar in any way. It satisfies both FH and Eggen's velocity criteria, lies in the middle of the main sequence in the CMD, and has no variability or binary observed in other surveys. A plausible scenario is that this star is a field star unassociated with the HR1614 moving group, but lies within the group's kinematical and photometric interval simply by chance. Out of our total sample of 18 stars we discover only the one star (if we disregard the other three stars assuming they are "confirmed" non-members or binaries) to be contaminating the HR1614 moving group. We are not aware of any literature calculations of the expected rate of contamination of moving groups.

In an attempt to estimate possible contamination, we obtained a synthetic stellar population based on Besancon models (Robin et al. 2003) with stars limited to the magnitude, color, and velocity criteria of the HR1614 group stars. The stellar sample was restricted to stars lying along the main sequence in Figure 7 with $4 < M_V < 7$ and $0.5 <$ B-V < 1.2, and width of Δ(B-V) $= \pm$ 0.2. The velocity space was restricted to stars lying along the tilt in Figure 5 with -55 $<$ U $<$ 25 km s^{-1} and -70 $<$ V $<$ -40 km s^{-1}, and width ΔV $= \pm$ 20 km s^{-1}. In this selected sample 15% of stars had solar-level metallicities as defined by [Fe/H] $= 0.00 \pm 0.05$. No prior restrictions were made on the metallicity. This suggests that one in seven stars from the background galactic disk in this restricted interval of absolute magnitude, color and velocity will have solar-level metallicity [Fe/H] $= 0.00 \pm 0.05$. We can therefore expect about one in seven such background stars in our HR 1614 moving group sample.

5.3. Implications for Chemical Tagging

The clear bimodal abundance pattern seen for the α, Fe, Fe-peak and light s-process elements is interesting. As discussed above, of the four deviating stars, only one cannot be classed as a non-member, a binary or otherwise peculiar star based on its kinematics or photometric properties. Although we are not aware of any prior calculation of the expected rate of contamination from field stars that are not part of the group, our simple estimate based on Besancon stellar population models show that some contamination (15%) is to be expected. It is likely that there are other such contaminating stars in this (and other) moving groups, that are not yet identified due to the lack of detailed chemical information. Our results are a clear demonstration of the necessity and importance of obtaining detailed chemical information, and that chemical probing is essential to see the true story behind the history of any stellar stream in the Galactic disk.

Our results support the conclusion of Feltzing & Holmberg (2000) regarding the reality of the HR 1614 moving group. Several authors have argued that at least some moving stellar groups are not the dispersed remnants of star-forming events, but rather are dynamical in origin, resulting from the dynamical effects of the galactic bar or spiral structure (eg. Dehnen 1999; De Simone et al. 2004; Famaey et al. 2005). We would not expect such dynamical groups to be coeval and chemically homogeneous. The homogeneity of the HR1614 group in age and abundance supports the view that this group is indeed the remnant of a dispersed star-forming event. Its kinematical coherence shows that such a dispersing system need not be significantly perturbed by external dynamical influences like galactic spiral structure or giant molecular clouds, at least over a period of order 2 Gyr.

Finally, the high level of chemical homogeneity observed across the confirmed HR1614 moving group members is a major step forward for chemical tagging. Earlier De Silva et al. (2006b) reported chemical homogeneity in the Hyades which is a younger bound star cluster. Our study on the very old open cluster Cr 261 (De Silva et al., in preparation) also show similar levels of homogeneity and in it we further explore the implications of our combined results on chemical tagging. Here we have shown that an unbound intermediate-aged cluster is also chemically identifiable. Although much work is yet to be done, the chemical tagging technique and the prospect of unravelling the dissipative history of the Galactic disk now seems viable.

GMD would like to thank Mary Williams for her assistance with determining radial and

space velocities, and Agris Kalnajs for useful discussions on the dynamics of stellar streams. We thank the anonymous referee for his helpful comments. This research has made use of the Vienna Atomic Line Database, operated at Vienna, Austria, and the Database on Rare Earths At Mons University, operated at Mons, Belgium.

REFERENCES

Allende Prieto, C., Asplund, M., López, R. J. G., & Lambert, D. L. 2002, ApJ, 567, 544

Allende Prieto, C., Barklem, P. S., Lambert, D. L., & Cunha, K. 2004, A&A, 420, 183

Alonso, A., Arribas, S., & Martinez-Roger, C. 1996, A&A, 313, 873

Barbier-Brossat, M., & Figon, P. 2000, A&AS, 142, 217

Bertelli, G., Bressan, A., Chiosi, C., Fagotto, F., & Nasi, E. 1994, A&AS, 106, 275

Biemont, E., Baudoux, M., Kurucz, R. L., Ansbacher, W., & Pinnington, E. H. 1991, A&A, 249, 539

Biemont, E., Palmeri, P., & Quinet, P. 1999, Astrophysics and Space Science, 635, 269

Castelli, F., Gratton, R. G., & Kurucz, R. L. 1997, A&A, 318, 841

De Silva, G. M., Freeman, k. C., Asplund, M., Bland-Hawthorn, J., Bessell, M. S., Garcia-Perez, A., & Collet, R. 2006a, submitted to AJ

De Silva, G. M., Sneden, C., Paulson, D. B., Asplund, M., Bland-Hawthorn, J., Bessell, M. S., & Freeman, K. C. 2006b, AJ, 131, 455

De Simone, R., Wu, X., & Tremaine, S. 2004, MNRAS, 350, 627

Dehnen, W. 1999, ApJ, 524, L35

Dehnen, W., & Binney, J. J. 1998, MNRAS, 298, 387

Den Hartog, E. A., Lawler, J. E., Sneden, C., & Cowan, J. J. 2003, ApJS, 148, 543

Eggen, O. J. 1978a, ApJ, 222, 191

—. 1978b, ApJ, 222, 203

—. 1992, AJ, 104, 1906

—. 1998, AJ, 115, 2453

Famaey, B., Jorissen, A., Luri, X., Mayor, M., Udry, S., Dejonghe, H., & Turon, C. 2005, A&A, 430, 165

Feltzing, S., & Holmberg, J. 2000, A&A, 357, 153

Freeman, K., & Bland-Hawthorn, J. 2002, ARA&A, 40, 487

Grenier, S., Baylac, M. O., Rolland, L., Burnage, R., Arenou, F., Briot, D., Delmas, F., Duflot, M., Genty, V., Gomez, A. E., Halbwachs, J.-L., Marouard, M., Oblak, E., & Sellier, A. 1999, VizieR Online Data Catalog, 413, 70451

Kupka, F., Piskunov, N. E., Ryabchikova, T. A., Stempels, H. C., & Weiss, W. W. 1999, A&AS, 138, 119

Kupka, F., Ryabchikova, T. A., Piskunov, N. E., Stempels, H. C., & Weiss, W. W. 2000, Baltic Astronomy, 9, 590

Kurtz, M. J., & Mink, D. J. 1998, PASP, 110, 934

Kurtz, M. J., Mink, D. J., Wyatt, W. F., Fabricant, D. G., Torres, G., Kriss, G. A., & Tonry, J. L. 1992, in ASP Conf. Ser. 25: Astronomical Data Analysis Software and Systems I, 432–+

Lawler, J. E., Wickliffe, M. E., den Hartog, E. A., & Sneden, C. 2001, ApJ, 563, 1075

Maurice, E., Mayor, M., Benz, W., Andersen, J., Nordström, B., Ardeberg, A., Lindgren, H., Imbert, M., Martin, N., & Prevot, L. 1984, A&AS, 57, 275

Nordström, B., Mayor, M., Andersen, J., Holmberg, J., Pont, F., Jørgensen, B. R., Olsen, E. H., Udry, S., & Mowlavi, N. 2004, A&A, 418, 989

Paulson, D. B., Sneden, C., & Cochran, W. D. 2003, AJ, 125, 3185

Piskunov, N. E., Kupka, F., Ryabchikova, T. A., Weiss, W. W., & Jeffery, C. S. 1995, A&AS, 112, 525

Prochaska, J. X., & McWilliam, A. 2000, ApJ, 537, L57

Prochaska, J. X., Naumov, S. O., Carney, B. W., McWilliam, A., & Wolfe, A. M. 2000, AJ, 120, 2513

Raboud, D., Grenon, M., Martinet, L., Fux, R., & Udry, S. 1998, A&A, 335, L61

Reddy, B. E., Tomkin, J., Lambert, D. L., & Allende Prieto, C. 2003, MNRAS, 340, 304

Robin, A. C., Reylé, C., Derrière, S., & Picaud, S. 2003, A&A, 409, 523

Ryabchikova, T. A., Piskunov, N. E., Stempels, H. C., Kupka, F., & Weiss, W. W. 1997, Baltic Astronomy, 6, 244

Skuljan, J., Cottrell, P. L., & Hearnshaw, J. B. 1997, in ESA SP-402: Hipparcos - Venice '97, 525–530

Smith, G. H. 1983, AJ, 88, 1775

Sneden, C., Kraft, R. P., Prosser, C. F., & Langer, G. E. 1992, AJ, 104, 2121

Sneden, C. A. 1973, Ph.D. Thesis

Turon, C., Creze, M., Egret, D., Gomez, A., Grenon, M., Jahreiß, H., Requieme, Y., Argue, A. N., Bec-Borsenberger, A., Dommanget, J., Mennessier, M. O., Arenou, F., Chareton, M., Crifo, F., Mermilliod, J. C., Morin, D., Nicolet, B., Nys, O., Prevot, L., Rousseau, M., Perryman, M. A. C., & et al. 1993, Bulletin d'Information du Centre de Donnees Stellaires, 43, 5

Yong, D., Carney, B. W., & de Almeida, M. L. T. 2005, AJ, 130, 597

Zwitter, T., Castelli, F., & Munari, U. 2004, A&A, 417, 1055

Table 1. Stellar Sample

HIP	HD	RA	DEC	V	B-V	V-K[a]	Source[b]
23311	32147	05 00 48.68	-05 45 03.5	6.22	1.05	2.51	E,FH
110996	213042	22 29 15.23	-30 01 06.3	7.65	1.08	2.53	E
26834	37986	05 41 53.54	-15 37 48.9	7.36	0.80	1.73	FH
109378	210277	22 09 29.82	-07 32 51.2	6.54	0.77	1.74	E,FH
22940	31452	04 56 10.61	-05 40 24.4	8.43	0.84	1.96	FH
116554	222013	23 37 15.31	-45 28 30.8	9.22	0.81	1.88	E,FH
10599	13997	02 16 27.60	+12 22 49.1	7.99	0.79	1.76	E,FH
110843	212708	22 27 24.38	-49 21 54.5	7.48	0.73	1.68	FH
17960	24040	03 50 22.90	+17 28 37.1	7.50	0.65	1.53	FH
22336	30562	04 48 36.20	-05 40 24.4	5.77	0.63	1.46	FH
102393	197623	20 44 57.03	+00 17 31.7	7.55	0.66	1.52	FH
11575	15590	02 29 11.90	-42 04 31.1	7.98	0.65	1.47	E
9353	12235	02 00 09.16	+03 05 49.2	5.89	0.61	1.40	E,FH
102018	196800	20 40 22.33	-24 07 04.9	7.21	0.61	1.42	FH
13513	18168	02 54 02.78	-35 54 16.8	8.23	0.93	2.36	FH
6762	8828	01 27 01.55	-00 09 27.3	7.96	0.74	1.80	E
116970	222655	23 42 42.22	-41 14 51.3	9.57	0.76	1.74	E
25840	36379	05 30 59.85	-10 04 49.1	6.94	0.56	1.39	E

[a]K magnitudes from 2MASS

[b]FH = Feltzing & Holmberg (2000), E = Eggen (1998)

Table 2. Line list

Wavelength(Å)	Species	LEP(eV)	log gf	EW(mÅ)	Wavelength(Å)	Species	LEP(eV)	log gf	EW(mÅ)	Wavelength(Å)	Species	LEP(eV)	log gf	EW(m
5688.19	Na I	2.11	−0.420	265.0	5618.63	Fe I	4.21	−1.292	75.0	4582.83	Fe II	2.84	−3.094	61.
6154.23	Na I	2.10	−1.530	128.0	5705.47	Fe I	4.30	−1.420	59.6	4620.52	Fe II	2.83	−3.079	39.
6160.75	Na I	2.10	−1.230	140.0	5741.85	Fe I	4.25	−1.689	64.0	4670.17	Fe II	2.58	−3.904	26.
5711.09	Mg I	4.35	−1.833	171.0	5778.45	Fe I	2.59	−3.480	58.9	5991.38	Fe II	3.15	−3.557	19.
6318.72	Mg I	5.11	−1.970	79.0	5811.92	Fe I	4.14	−2.430	25.5	6084.11	Fe II	3.20	−3.808	10.
6696.02	Al I	3.14	−1.340	110.0	5837.70	Fe I	4.29	−2.340	29.0	6149.26	Fe II	3.89	−2.724	16.
6698.67	Al I	3.14	−1.640	84.3	5853.16	Fe I	1.49	−5.280	41.6	6247.56	Fe II	3.89	−2.329	22.
7835.31	Al I	4.02	−0.470	125.0	5856.10	Fe I	4.29	−1.640	60.5	6416.92	Fe II	3.89	−2.740	37.
7836.13	Al I	4.02	−0.310	148.8	5858.79	Fe I	4.22	−2.260	28.1	6432.68	Fe II	2.89	−3.708	28.
5665.56	Si I	4.92	−1.940	50.5	5927.80	Fe I	4.65	−1.090	64.5	6456.38	Fe II	3.90	−2.075	30.
5684.49	Si I	4.95	−1.550	67.0	5956.69	Fe I	0.86	−4.608	102.5	7224.49	Fe II	3.89	−3.243	17.
5690.43	Si I	4.93	−1.770	55.0	6054.08	Fe I	4.37	−2.310	26.0	7711.72	Fe II	3.90	−2.543	33.
5948.54	Si I	5.08	−1.230	90.6	6120.24	Fe I	0.91	−5.970	40.0	5846.99	Ni I	1.68	−3.210	70.
6142.48	Si I	5.62	−1.540	32.8	6151.62	Fe I	2.17	−3.299	83.0	6086.28	Ni I	4.26	−0.515	65.
6145.01	Si I	5.62	−1.362	40.5	6157.73	Fe I	4.08	−1.320	87.4	6175.37	Ni I	4.09	−0.535	68.
6155.13	Si I	5.62	−0.786	83.2	6180.20	Fe I	2.73	−2.637	101.5	6177.24	Ni I	1.83	−3.510	46.
5868.57	Ca I	2.93	−1.570	79.5	6200.31	Fe I	2.61	−2.437	120.0	6204.60	Ni I	4.09	−1.140	42.
6169.04	Ca I	2.52	−0.797	211.5	6219.28	Fe I	2.20	−2.433	148.5	6635.12	Ni I	4.42	−0.828	40.
6169.56	Ca I	2.53	−0.478	261.0	6229.23	Fe I	2.84	−2.846	69.0	6772.32	Ni I	3.66	−0.987	73.
6455.60	Ca I	2.52	−1.290	121.2	6246.32	Fe I	3.60	−0.894	215.0	4050.33	Zr II	0.71	−1.000	33.
6572.80	Ca I	0.00	−4.280	115.0	6265.13	Fe I	2.17	−2.550	149.0	5853.69	Ba II	0.60	−1.000	75.
6013.53	Mn I	3.07	−0.251	168.7	6270.22	Fe I	2.86	−2.500	84.5	6141.73	Ba II	0.70	−0.076	148
6016.67	Mn I	3.08	−0.100	170.6	6271.28	Fe I	3.33	−2.728	57.8	6496.91	Ba II	0.60	−0.410	115
6021.80	Mn I	3.08	0.034	176.8	6297.79	Fe I	2.22	−2.740	114.5	4083.22	Ce II	0.70	0.270	..
4139.93	Fe I	0.99	−3.629	126.0	6336.82	Fe I	3.68	−0.916	193.0	4137.65	Ce II	0.52	0.440	..
4216.19	Fe I	0.00	−3.356	400.0	6411.65	Fe I	3.65	−0.734	232.5	4364.65	Ce II	0.49	0.230	..
4232.72	Fe I	0.11	−4.928	121.0	6574.23	Fe I	0.99	−5.004	83.0	4562.36	Ce II	0.48	0.230	..
4347.24	Fe I	0.00	−5.503	83.5	6609.11	Fe I	2.56	−2.692	118.0	4628.16	Ce II	0.52	0.200	..
4389.24	Fe I	0.05	−4.583	116.0	6699.16	Fe I	4.59	−2.170	20.5	4012.24	Nd II	0.63	0.810	..
4439.88	Fe I	2.28	−3.002	70.5	6739.52	Fe I	1.56	−4.820	49.0	4012.69	Nd II	0.00	−0.600	..
4442.34	Fe I	2.19	−1.255	339.5	6810.26	Fe I	4.60	−1.000	80.3	4068.89	Nd II	0.00	−1.420	..
4445.48	Fe I	0.08	−5.441	85.0	4178.86	Fe II	2.57	−2.720	87.0	4462.98	Nd II	0.56	0.040	..
4489.74	Fe I	0.12	−3.966	189.0	4491.41	Fe II	2.86	−2.684	63.0	4129.23	Eu II	0.00	0.270	..
4531.15	Fe I	1.48	−2.155	295.0	4508.28	Fe II	2.86	−2.312	64.5	...	...	...	...	..
4602.01	Fe I	1.61	−3.154	108.6	4576.33	Fe II	2.84	−2.822	48.0	...	...	...	...	..

Table 3. Adopted Stellar Parameters

HIP	Mass ($M_\odot$)	M_{bol}	T_{eff}(K)	log g(cm s^{-2})	ξ(km s^{-1})
23311	0.80	6.34	4850	4.4	0.8
110996	0.78	6.34	4800	4.3	0.8
26834	0.95	5.33	5500	4.3	0.7
109378	0.97	5.25	5500	4.3	0.7
22940	0.93	5.50	5250	4.5	0.4
116554	0.92	5.50	5400	4.7	0.6
10599	0.95	5.33	5450	4.5	1.0
110843	1.00	5.00	5600	4.3	1.1
17960	1.12	4.32	5800	4.4	1.1
22336	1.25	3.70	5900	4.4	1.3
102393	1.20	3.80	5900	4.4	1.1
11575	1.30	3.20	5900	4.1	1.2
9353	1.30	3.45	6000	4.2	1.2
102018	1.20	4.14	6000	4.4	1.2
13513	0.87	5.90	5050	4.5	1.1
6762	0.95	5.17	5400	4.6	0.9
116970	0.97	5.17	5500	4.7	0.9
25840	1.25	3.85	6150	4.5	1.2

Table 4. Absolute Abundances (log ϵ)

HIP ID	Na	Mg	Al	Si	Ca	Mn	Fe	Ni	Zr	Ba	Ce	Nd	Eu
23311	6.56	7.86	6.77	7.78	6.65	5.79	7.77	6.63	2.72	2.52	1.75	1.58	0.74
110996	6.61	7.83	6.73	7.77	6.67	5.79	7.75	6.57	2.65	2.51	1.68	1.53	0.71
26834	6.62	7.98	6.72	7.90	6.71	5.82	7.83	6.69	2.77	2.67	1.74	1.56	0.71
109378	6.50	7.92	6.65	7.83	6.60	5.72	7.76	6.55	2.77	2.61	1.73	1.56	0.76
22940	6.41	7.87	6.60	7.79	6.60	5.76	7.75	6.63	2.94	2.59	1.73	1.58	0.73
116554	6.35	7.78	6.52	7.77	6.55	5.73	7.75	6.54	2.73	2.56	1.73	1.62	0.71
10599	6.54	7.82	6.68	7.88	6.59	5.73	7.77	6.64	2.83	2.52	1.72	1.57	0.68
110843	6.55	7.84	6.65	7.83	6.59	5.76	7.79	6.58	2.73	2.51	1.71	1.55	0.71
179690	6.49	7.87	6.64	7.78	6.58	5.72	7.72	6.59	2.72	2.55	1.75	1.56	0.74
22336	6.48	7.78	6.59	7.83	6.56	5.74	7.76	6.57	2.77	2.62	1.73	1.56	0.73
102393	6.57	7.80	6.64	7.88	6.61	5.76	7.82	6.63	2.79	2.60	1.74	1.53	0.76
11575	6.58	7.80	6.57	7.81	6.55	5.73	7.77	6.56	2.75	2.60	1.68	1.56	0.76
9353	6.61	7.76	6.61	7.87	6.57	5.74	7.73	6.57	2.72	2.53	1.67	1.56	0.74
102018	6.51	7.76	6.51	7.76	6.59	5.73	7.72	6.53	2.73	2.51	1.64	1.55	0.78
13513	6.17	7.61	6.34	7.59	6.38	5.39	7.55	6.31	2.44	2.33	1.55	1.43	0.61
6762	6.06	7.47	6.24	7.53	6.25	5.32	7.47	6.21	2.51	2.41	1.61	1.41	0.61
116970	6.20	7.63	6.27	7.61	6.38	5.38	7.55	6.32	2.50	2.46	1.67	1.44	0.65
25840	6.16	7.61	6.24	7.47	6.27	5.36	7.44	6.21	2.51	2.42	1.59	1.42	0.65

Table 5. Abundance Sensitivities

Example Star	Model Parameter	Na	Mg	Al	Si	Ca	Mn	Fe	Ni	Zr	Ba	Ce	Nd	Eu
HR1614	$T_{\rm eff}$±50	±0.04	±0.01	±0.03	∓0.02	±0.03	0.00	±0.02	∓0.01	±0.01	±0.01	±0.02	±0.01	±0.01
($T_{\rm eff}$ = 4850K)	log g±0.1	∓0.05	∓0.02	∓0.04	±0.01	∓0.04	0.00	0.00	±0.01	±0.04	0.00	0.00	0.00	±0.03
	ξ±0.1	∓0.01	∓0.02	∓0.02	∓0.01	∓0.04	±0.02	∓0.04	∓0.03	∓0.05	∓0.05	±0.01	±0.02	0.00
	Δ EW / synth	±0.03	±0.06	±0.05	±0.04	±0.03	±0.03	±0.03	±0.03	±0.02	±0.02	±0.02	±0.02	±0.02
HIP9353	$T_{\rm eff}$±50	±0.02	±0.02	±0.02	∓0.01	±0.02	±0.01	±0.04	±0.01	0.00	±0.01	±0.01	0.00	±0.01
($T_{\rm eff}$ = 6000K)	log g±0.1	∓0.02	∓0.01	∓0.01	0.00	∓0.01	0.00	∓0.01	0.00	±0.04	±0.01	±0.01	±0.02	±0.03
	ξ±0.1	∓0.02	∓0.02	∓0.01	∓0.03	∓0.04	±0.02	∓0.03	∓0.04	∓0.04	∓0.05	0.00	0.00	±0.01
	Δ EW /synth	±0.04	±0.05	±0.06	±0.04	±0.02	±0.03	±0.01	±0.04	±0.02	±0.02	±0.02	±0.02	±0.02

Table 6. Radial Velocities

HIP ID	This study	N04	FH sources*
23311	21.6	21.0	27.0
110996	5.3	4.8	7.4
26834	59.1	···	67.0
109378	-21.3	···	-24.1
22940	15.2	···	14.3
116554	-16.5	-15.1	-2.6
10599	-21.5	-21.3	-23.6
110843	4.7	4.9	-7.3
17960	-10.1	···	-7.6
22336	76.7	77.0	78.6
102393	-69.2	···	-71.0
11575	37.0	36.9	36.8
9353	-18.1	-18.5	-18.4
102018	-63.5	-63.8	-61.2
13513	3.5/-46.9	4.0	3.0
6762	13.7	13.2	3.5
116970	27.7	···	26.9
25840	22.9	22.8	···

RV standards:		This study	Maurice et al. (1984)
	HD6677	19.7	19.5
	CPD432527	20.0	19.1

*Turon et al. (1993); Barbier-Brossat & Figon (2000); Grenier et al. (1999)

Table 7. UVW Velocities

HIP ID	U	V	W	U(FH)	V(FH)	W(FH)
23311	14.9	-49.7	-3.8	10.65	-51.83	-6.33
110996	15.6	-54.7	-7.8	16.55	-54.51	-9.70
26834	-21.6	-56.3	6.2	-27.11	-61.11	3.02
109378	13.9	-45.4	2.9	12.46	-46.78	3.09
22940	15.2	-56.7	-3.1	15.40	-56.50	-3.05
116554	1.0	-53.3	28.1	3.27	-54.08	17.25
10599	10.9	-50.2	11.9	12.00	-50.73	13.64
110843	-29.3	-62.1	-12.7	-35.96	-60.25	-2.93
17960	21.1	-54.2	-7.3	20.26	-53.93	-7.57
22336	-41.8	-67.7	-13.8	-43.26	-68.33	-14.98
102393	-45.3	-54.4	-3.4	-47.02	-55.19	-3.02
11575	14.7	-51.7	6.6	···	···	···
9353	11.7	-48.6	12.3	11.55	-48.59	12.43
102018	-50.6	-66.9	-1.4	-48.95	-65.96	-2.84
13513	-14.5/-3.1	-59.7/-39.8	38.6/83.3	-14.75	-59.61	39.00
6762	-3.9	-53.8	-22.1	-4.09	-53.95	-22.13
116970	9.9	-55.7	-16.2	9.87	-55.64	-15.42
25840	19.8	-70.6	-7.0	···	···	···

Table 8. Mean Abundances and Scatter

Element	⟨Members⟩	σ	⟨All Stars⟩	σ
Fe	7.77	0.033	7.71	0.117
Na	6.53	0.078	6.44	0.178
Mg	7.83	0.063	7.77	0.125
Al	6.63	0.075	6.55	0.169
Si	7.82	0.047	7.76	0.126
Ca	6.60	0.046	6.53	0.130
Mn	5.75	0.030	5.67	0.169
Ni	6.59	0.046	6.52	0.148
Zr	2.76	0.067	2.70	0.129
Ba	2.56	0.051	2.52	0.085
Ce	1.71	0.034	1.69	0.059
Nd	1.56	0.022	1.53	0.062
Eu	0.73	0.027	0.71	0.051

Table 9. Intrinsic scatter

Element	σ_{int}	uncertainty
Fe	0.000	0.010
Na	0.034	0.050
Mg	0.000	0.020
Al	0.017	0.040
Si	0.000	0.017
Ca	0.000	0.020
Mn	0.000	0.010
Ni	0.009	0.010
Zr	0.000	0.030
Ba	0.000	0.025
Ce	0.016	0.020
Nd	0.000	0.010
Eu	0.000	0.018

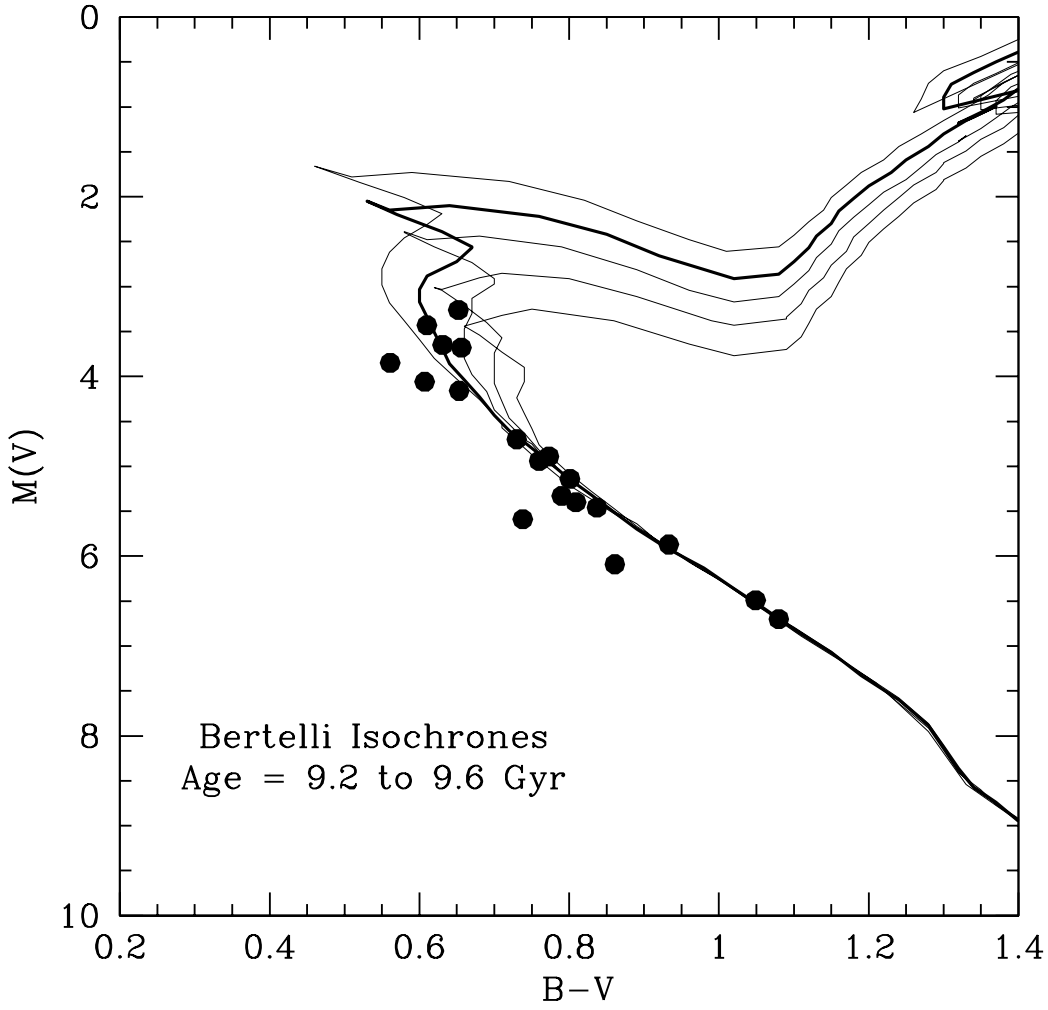

Fig. 1.— Our sample stars overlaid with Bertelli et al. (1994) isochrones. The best fitting isochrone of ≈ 2 Gyr is highlighted. Note all isochrones are for Z = 0.05.

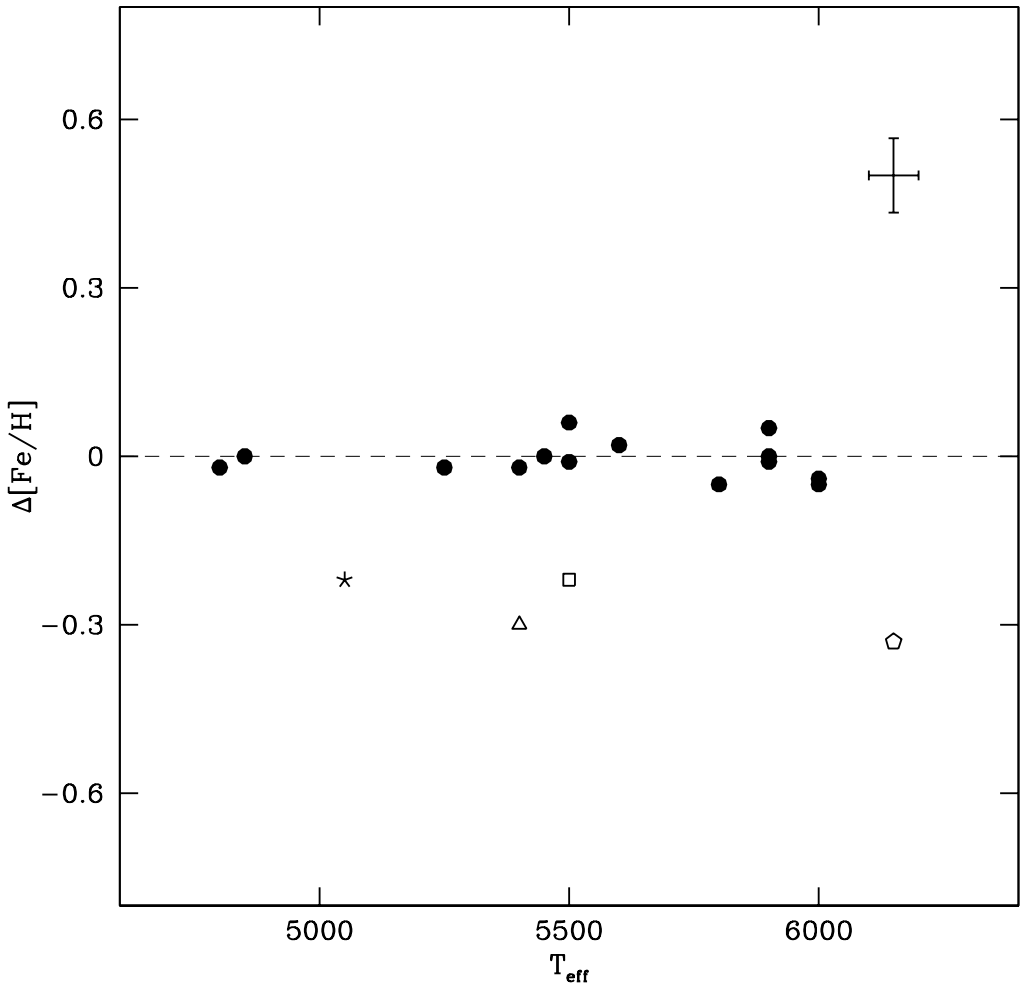

Fig. 2.— Differential Fe abundances. Typical errors are shown in the top right. Note that the y-axis zero level corresponds to the abundance of star HR1614, and does not represent the solar level as our abundances are calculated relative to HR1614. The majority of the sample (filled circles) are metal rich with [Fe/H] ≈ 0.25 dex. The lower four stars have solar metallicities. These stars are HIP13513 (star), HIP6762 (triangle), HIP25840 (hexagon) and HIP116970 (square). The membership probabilities of these stars are discussed in Section 5.2.

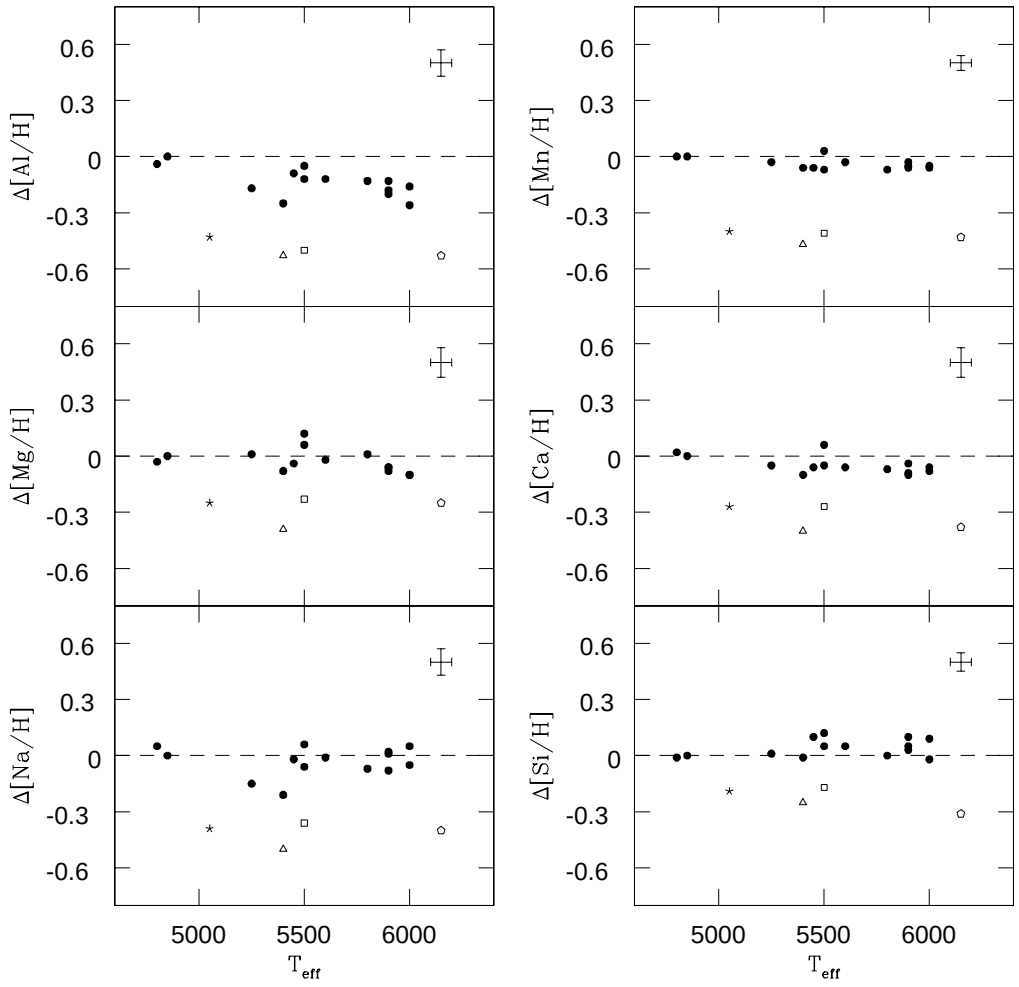

Fig. 3.— Differential abundances relative to HR1614 for elements up to Mn. The symbols are the same as those for Fig 2. The bimodality seen in Fig 2 is clearly present in these elements as well.

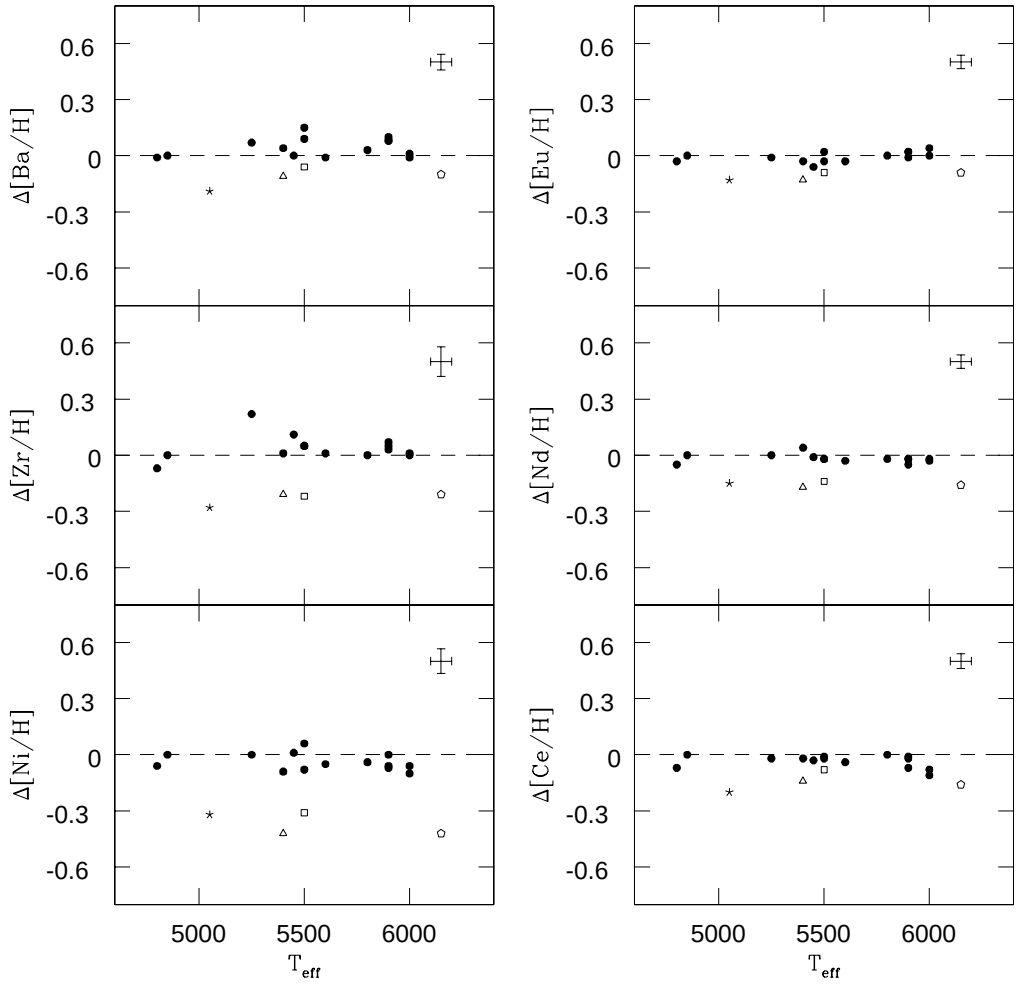

Fig. 4.— Differential abundances relative to HR1614 for elements heavier than Fe. The symbols are the same as those for Fig 2. While a clear bimodality is observed for Ni and Zr, the two groups tend to converge for the heavier s- and r- process elements.

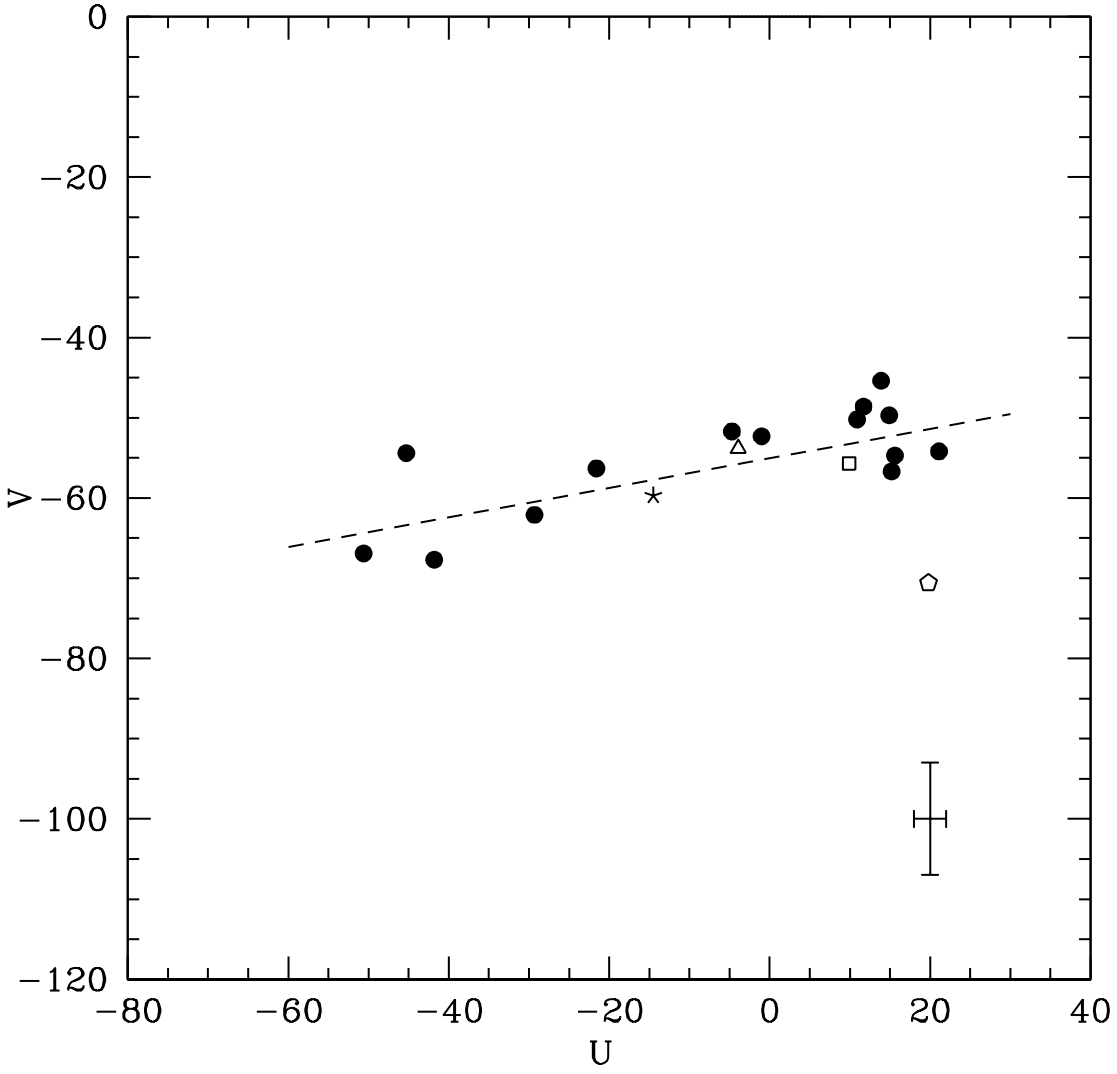

Fig. 5.— The derived UV velocities of the sample stars. Note the chemically deviating stars are identified with different symbols as in Fig 2. The dashed line represents the line of best fit. Typical errors are shown on the bottom right corner.

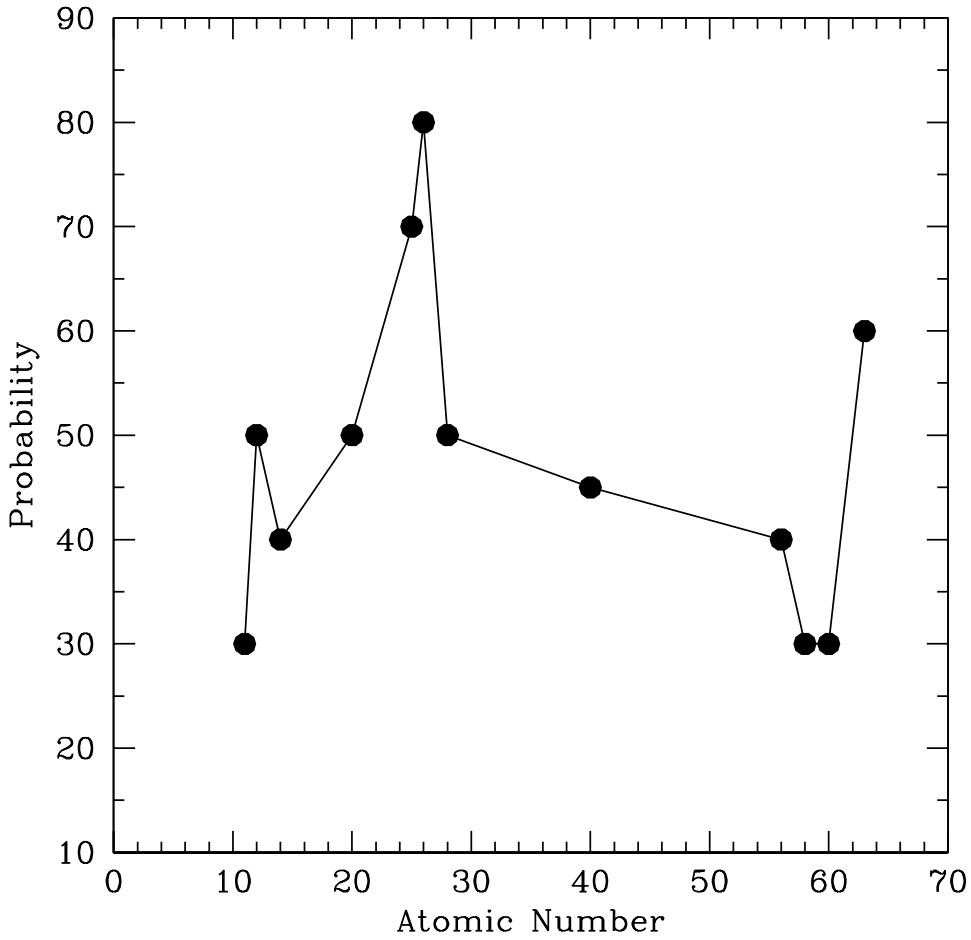

Fig. 6.— The probability of finding a scatter as large as observed given the measuring errors and zero intrinsic scatter for the studied elements. Fe (N = 26) is the element most consistent with zero intrinsic scatter.

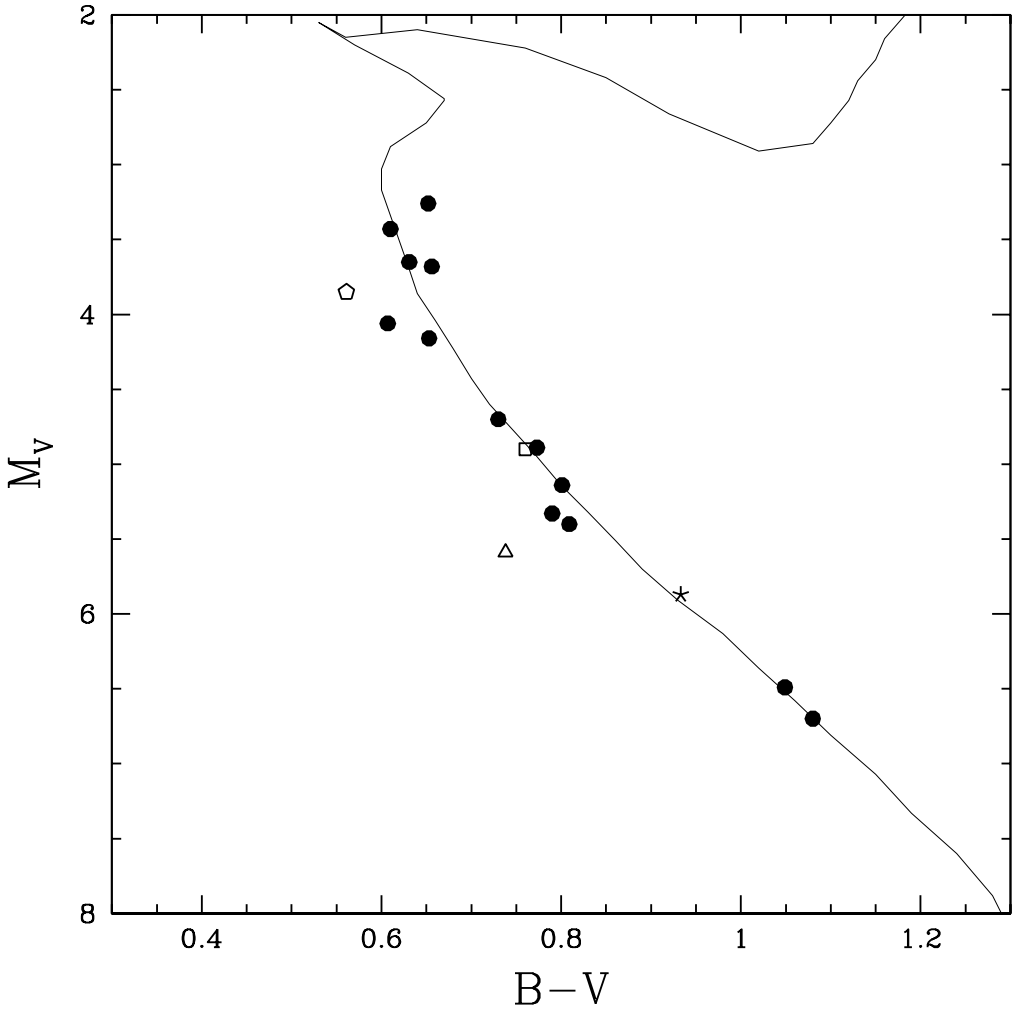

Fig. 7.— V vs. B-V color-magnitude diagram for our sample stars. The chemically deviating stars are identified with symbols as in Fig 2. The best fitting 2 Gyr Bertelli et al. (1994) isochrone with Z = 0.05 has been overlaid to guide the eye.